MNRAS 000, 1–12 (2015) Preprint 16 September 2022 Compiled using MNRAS LaTeX style file v3.0

Kelvin-Helmholtz MHD instabilities of supersonic shear layers with heat flux in anisotropic space plasmas

N. S. Dzhalilov,[1★] R. Ismayilli,[2]
[1] *Shamakhy Astrophysical Observatory, Shamakhy, Azerbaijan*
[2] *Center for Mathematical Plasma-Astrophysics, KU Leuven, Leuven, Belgium*

Accepted XXX. Received YYY; in original form ZZZ

ABSTRACT
The linear MHD Kelvin-Helmholtz instability (KHI) in an anisotropic plasma is studied. The governing equations obtained as the 16 moments of Boltzmann-Vlasov kinetic equations including the heat flow are applied. In the case of tangential discontinuity between the supersonic flows along the magnetic field calculated growing rates as functions of the anisotropic plasma properties allow us to conclude that quasi-transverse modes grow faster. Then dispersion equations for the KHI of quasi-transverse modes are derived considering the finite width of the transition zone with different velocity profiles. For these modes, when the role of heat flow is not important, the plasma parameters are controlled so that the fundamental plasma instabilities (firehose and mirror) do not affect the KHI. The problem is solved analytically, which is essential for numerical simulation. In contrast to the tangential discontinuity, the finite width of the transition layer confines KHI excitation as the wavenumber increases. In the general case of oblique propagation (when a heat flux complicates the problem), the boundary value problem is solved to determine the spectral eigenvalues. In particular, it is observed that fundamental plasma instabilities that arise in the transition zone between flows with a finite width can modify and considerably enhance KHI.

Key words: Solar wind, plasmas, MHD, turbulence, waves

Agenda

- Introductory remarks, formulation of the problem
- Boltzmann-Vlasov kinetic equations and their integrated 16-moments as a system of MHD transport equations
- Large-scale instabilities in an anisotropic collisionless plasma
- Shear MHD KHI instability in an anisotropic plasmas
- MHD instabilities as a energy source of the large-scale turbulence
- Conclusions

WHAT IS STABILITY?

- We can study a variable as a function of time to see how it behaves.
  - Perhaps this is the amplitude of a wave, and we want to see if it grows or dies.
  - Or, it could be the temperature or pressure, etc., of a system.
- Stability happens when a perturbation causes a restoring force that cancels the perturbation.
  - Guitar String
  - Ball in a bowl
  - Ocean Waves
  - Alfvén Waves (Sometimes)
- Instability happens when a perturbation causes a force that reinforces that perturbation.
  - Ball rolling off a hill
  - Kelvin-Helmholtz
  - Rayleigh Taylor
  - Magnetorotational

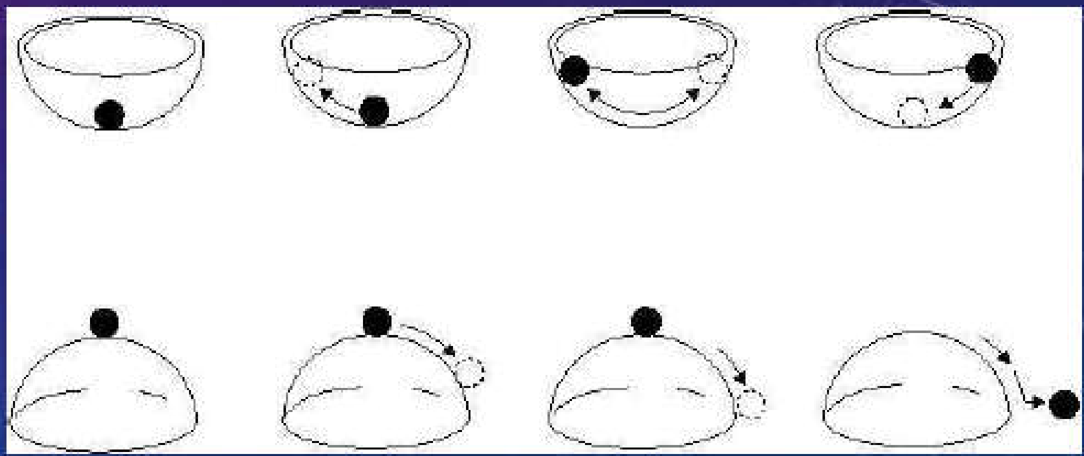

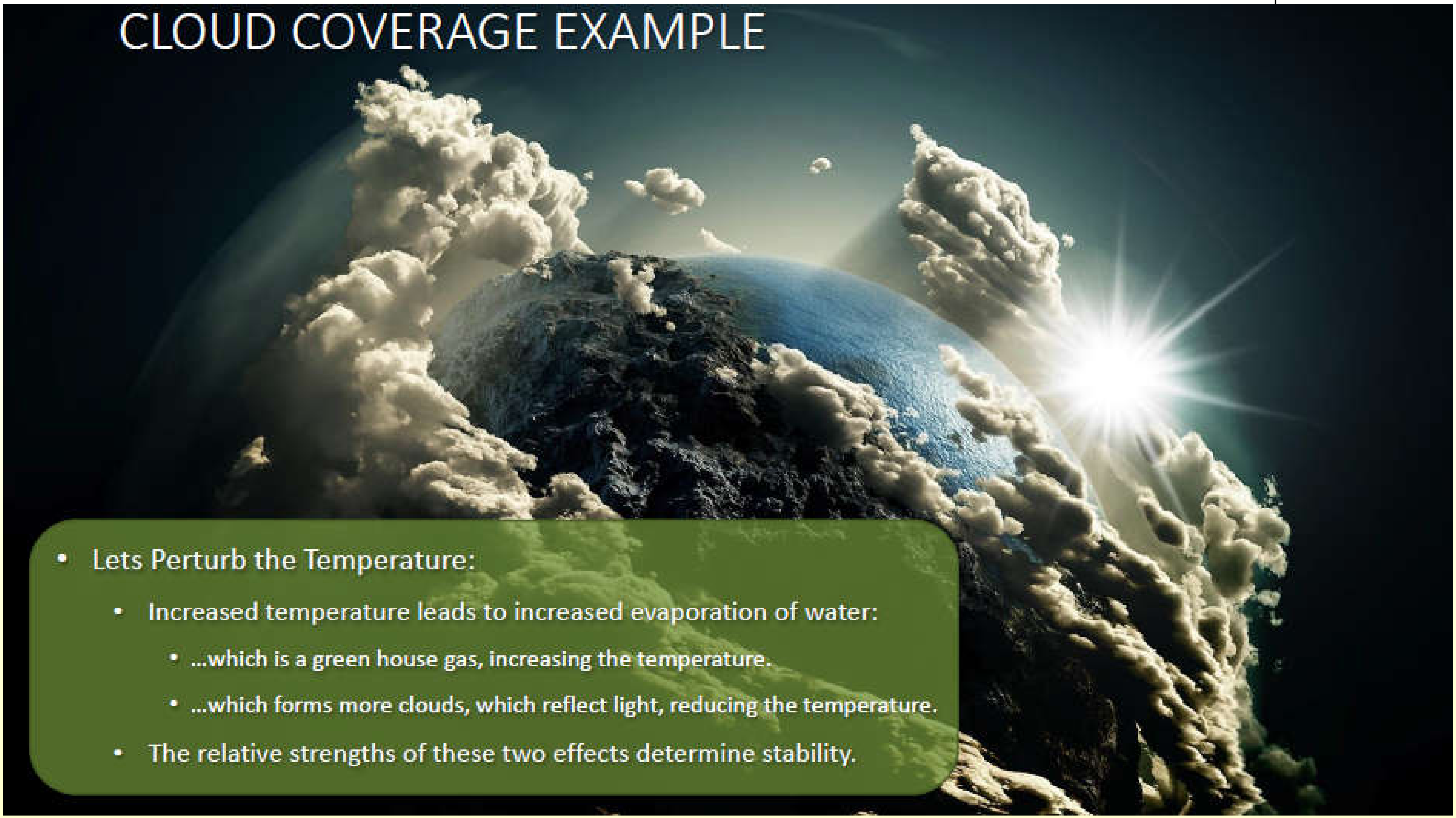
CLOUD COVERAGE EXAMPLE
• Lets Perturb the Temperature:
• Increased temperature leads to increased evaporation of water:
• ...which is a green house gas, increasing the temperature.
• ...which forms more clouds, which reflect light, reducing the temperature.
• The relative strengths of these two effects determine stability.

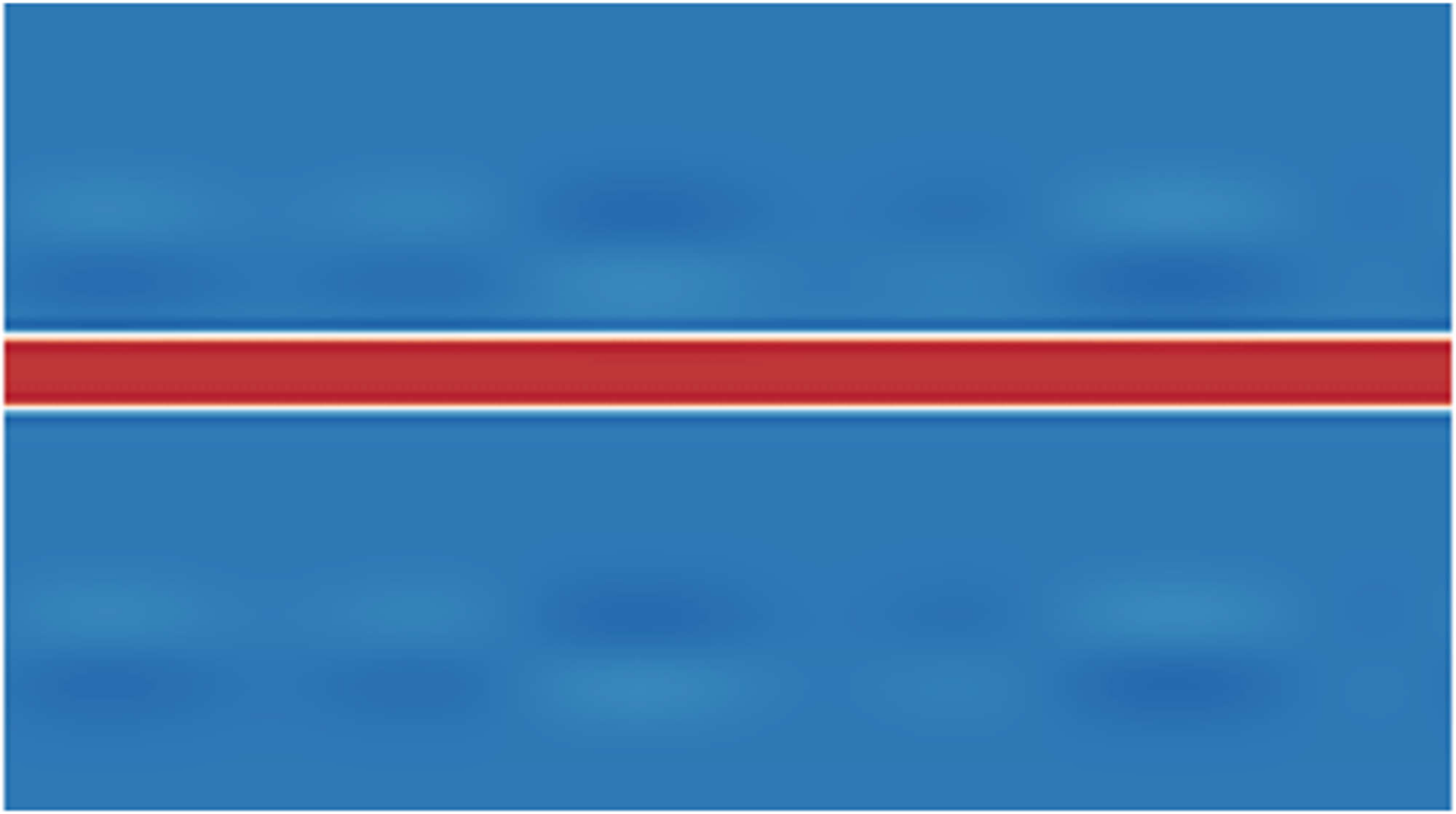

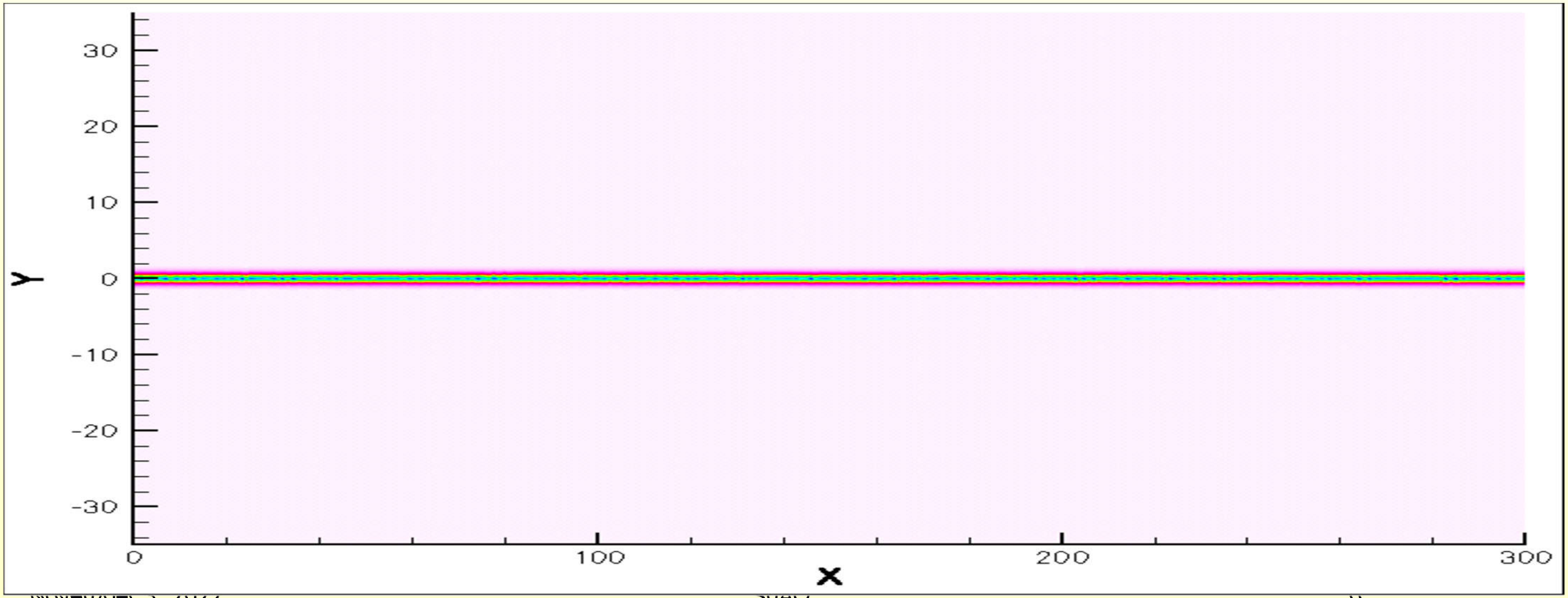

Y
30
20
10
0
-10
-20
-30
X
0
100
200
300

Kelvin-Helmholtz instability in the solar corona, solar wind and in geomagnetosphere.

V.V. Mishin, V.M. Tomozov ISTP Sb RAS Irkutsk

KHI is most is the most common and most strong instability in nature. Some examples.

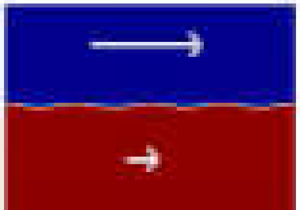

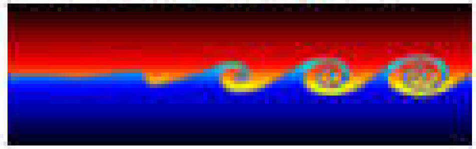

White caps on the water, overturning wave

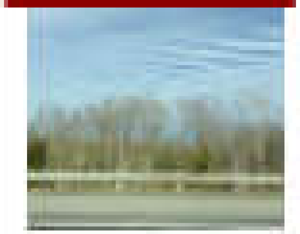

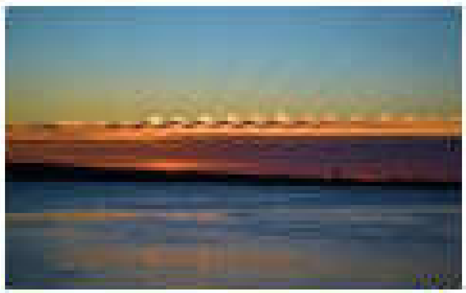

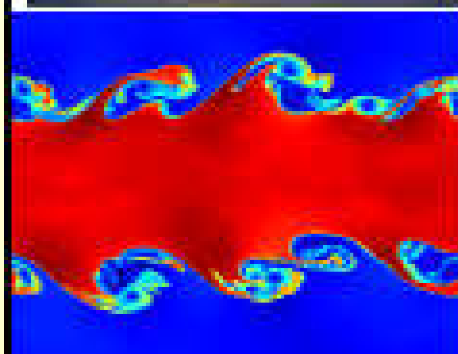

development of KHI of the jet with two boundaries or cylindrical jet gives formation of vortices on both jet borders - Karman road. Airplane and flamethrower jets disappear due to KHI development- diffusive widening.

Pacific typhoon

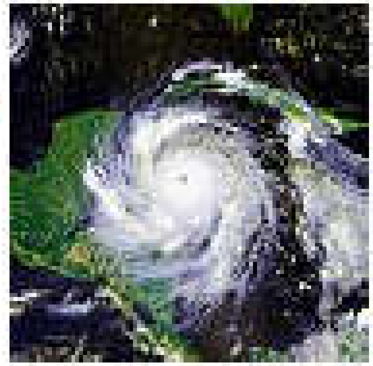

Atlantic hurricane

Spiral structure of atmospheric cyclones, heliospheric current layer and spiral arms of a galaxies - is possible KHI manifestation in rotational velocity shear-due to sharp change of angular velocity

Heliosphere

Galaxy spiral arms

Manifestations KHI in spac
e.K-H I in Solar corona

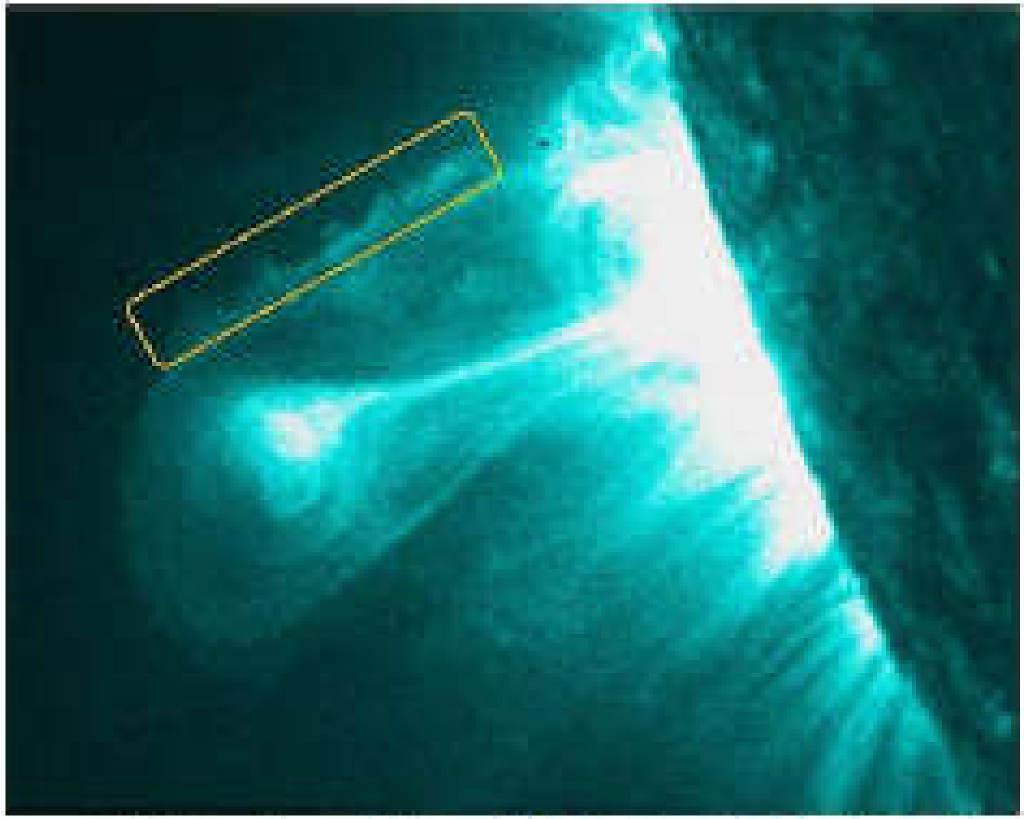

Foullon et al (Astrophys. J. Letts. 729:L8 (4pp), 2011 March1)

Fast coronal mass ejecta erupting from the Sun, with KH waves detected on its northern flank.

The *Solar Dynamics Observatory/Atmospheric Imaging Assembly* (SDO/AIA) image, shown in solar centered X (increasing toward west) vs Y (increasing toward north) coordinates, is taken in 131 Å channel. The overlaid rectangular region of interest indicates the northern flank region, where substructures, corresponding to the presumed KH waves, are detected against the darker coronal background.

Saturn’s atmosphere

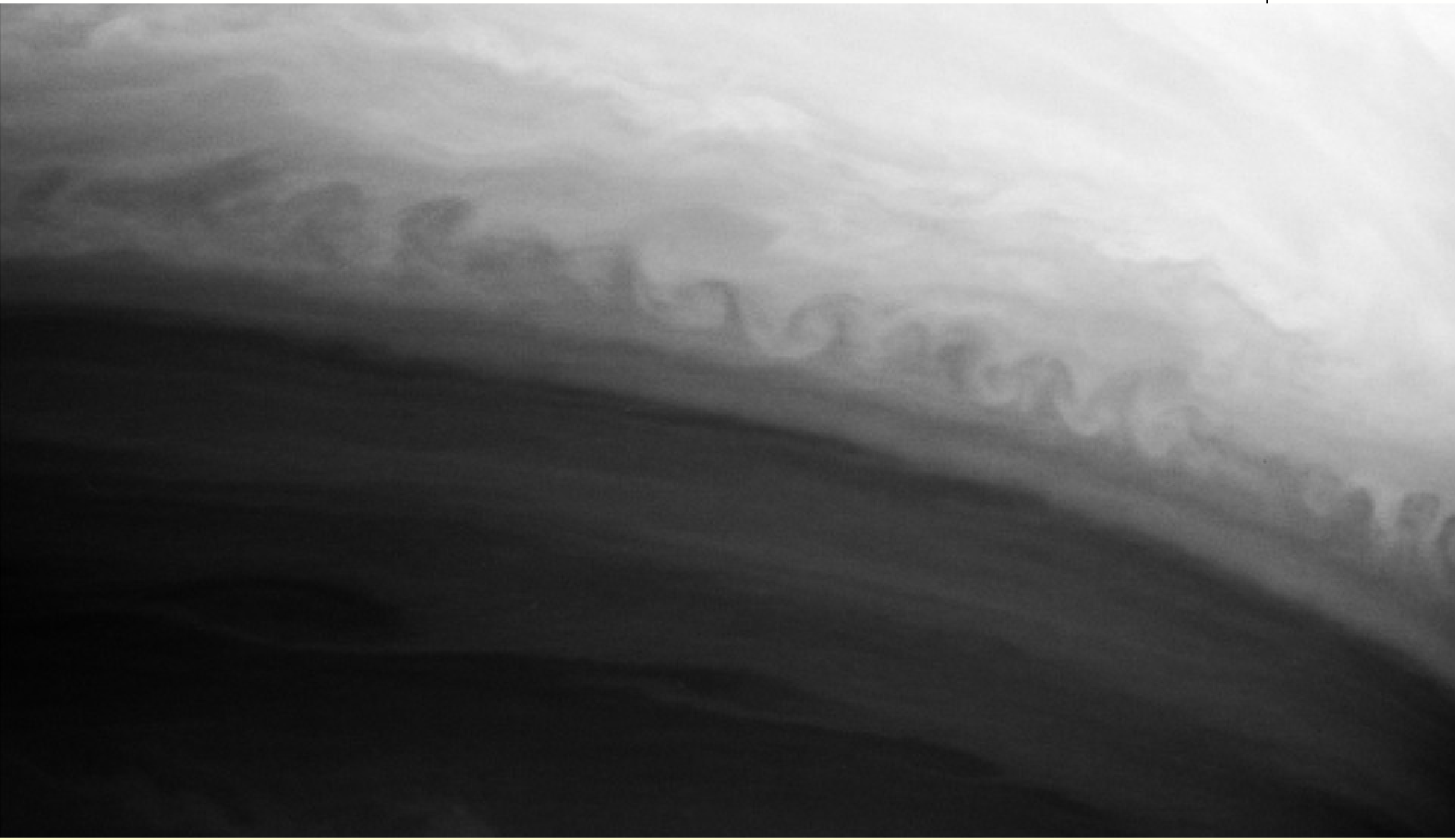

KEY EQUATIONS FOR KELVIN-HELMHOLTZ

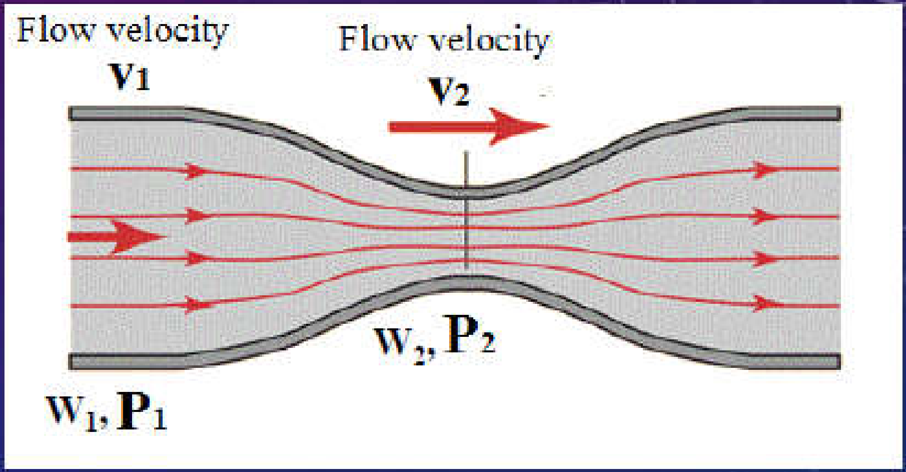

- *Continuity Equation*
  - $\rho_1 v_1 W_1 = \rho_2 v_2 W_2$
    - Assume $\rho_1 = \rho_2$:
    - $v_2 = v_1 \frac{W_1}{W_2}$
    - As channel width decreases, velocity increases.
- *Bernoulli Equation*
  - $P + \rho g h + \frac{1}{2}\rho v^2 = P_0 = constant$
  - Call g = 0 :
    - $P = P_0 - \frac{1}{2}\rho v^2$
    - As velocity increases, pressure decreases.

Together, this says that
a constriction in the flow will decrease the pressure.

Kelvin-Helmholtz instability **(K-H I)** develops on a tangential discontinuity (**TD**) - thin boundary between two flows having different velocities.
Example: wind instability at the surface of a sea.
Also it is called *the velocity shear instability.*
It was described by **Helmholtz (1868)** and **Kelvin (1871).**
Nature of instability: initiation of wing lift by concentration of streamlines over random boundary displacement. Increase of dynamic pressure $\rho V^2/2$ according to Bernoulli theorem: $P + \rho V^2/2 + \rho gz = const$
causes decompression over the displaced boundary $\Delta P = -\Delta\rho\upsilon^2/2 = -\rho\mathbf{\upsilon}\cdot\Delta\mathbf{\upsilon}$
which forces initial displacement to grow more, $md\mathbf{V}z/dt = \mathbf{F}_z = -\nabla P = \rho(\mathbf{\upsilon}\cdot\nabla)\mathbf{\upsilon} > 0$
so initial convexity (and concavity also) increases with time.

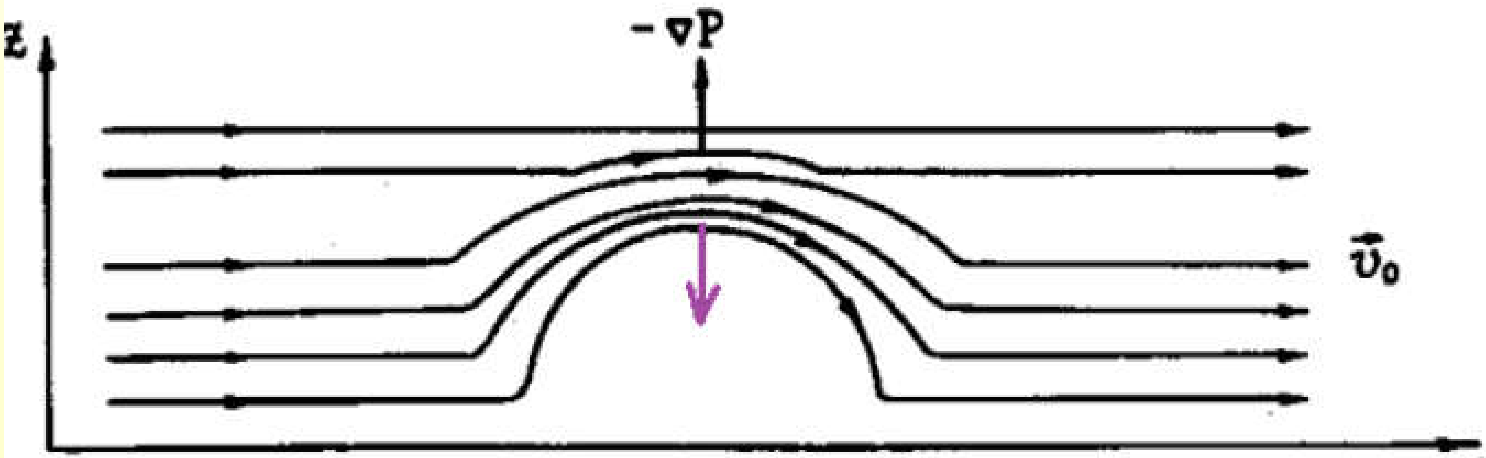

surface capillar and Maxwell tension forces

Helmholtz (1868), Kelvin (1871)

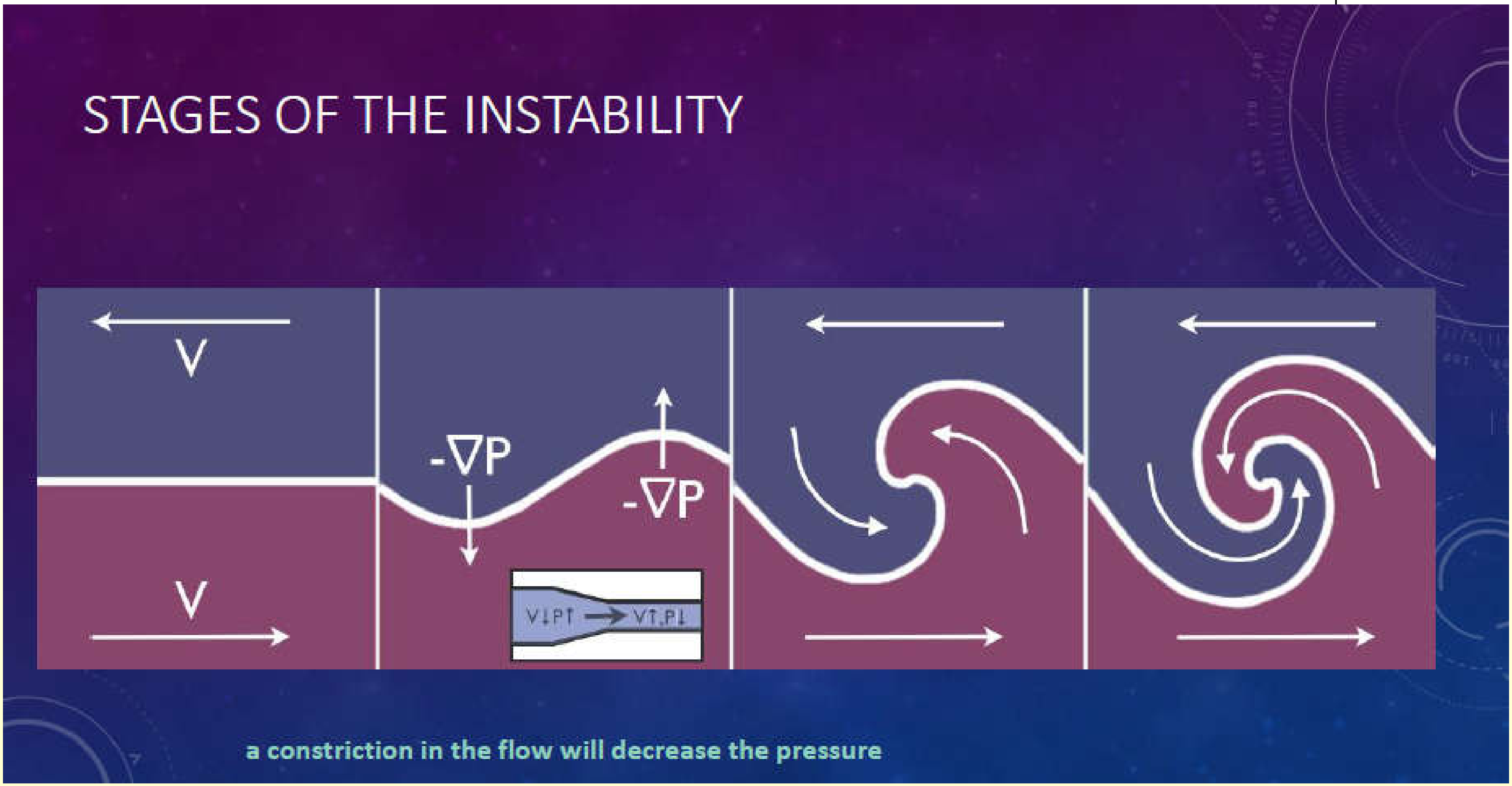

Conditions in the solar corona: strongly magnetized, anisotropic, rarefied and almost collisionless hot plasma

$T_e \approx T_i = 10^6$ K; $V_{Te} \approx 4000$ km s^{-1}, $V_{Ti} \approx 100$ km s^{-1},
$n_e = n_p \approx 10^9$ cm^{-3}; $2\pi/\omega_{pe} \approx 3{,}5 \times 10^{-9}$ s, $2\pi/\omega_{pi} \approx 1{,}5 \times 10^{-7}$ s
$B \approx 0.1 \div 100$ G; $2\pi/\omega_{Be} \approx 10^{-6} \div 10^{-9}$ s; $2\pi/\omega_{Bi} \approx 10^{-2} \div 10^{-5}$ s

$\tau_{ee} \approx 7{,}5 \times 10^{-6}$ s, $\tau_{ii} \approx 3.2 \times 10^{-4}$ s, $\tau_{ei} \approx 10^{-2}$ s
$\lambda_{ee} \approx \lambda_{ii} \approx 3000$ cm, $\lambda_{ei} \approx 40$ km

$r_{Be} \approx 200 \div 0.2$ cm, $r_{Bi} \approx 9000 \div 9$ cm
$\tau_{Be} \approx 10^{-6} \div 10^{-9}$ s, $\tau_{Bi} \approx 10^{-2} \div 10^{-5}$ s

Approach of a strong field: $\lambda_{ee} >> r_{Be}$, $\lambda_{ii} >> r_{Bi}$, $\tau_{ee} >> \tau_{Be}$, $\tau_{ii} >> \tau_{Bi} \Rightarrow$
There is no "mixing" of transverse and longitudinal energy: $f = f(v_{||}, v_{\perp}, \mathbf{r}, t)$

Anisotropy: $$\alpha = \frac{p_\perp}{p_\|} = \frac{T_\perp}{T_\|} \neq 1$$

There are observations in the solar wind ($\alpha \sim 2 \div 3$), in the outer corona ($\alpha > 100$) for heavy ions and protons, and in a coronal hole ($\alpha \sim 10$).

Moreover: $V_A \approx 10 \div 10^4$ km s^{-1}, $C_s = V_{Ti} \approx 100$ km s^{-1}.
$V_{turb} \approx 25 \div 50$ km s^{-1} (turbulence) from the non-thermal broadening of line profiles;
plasma parameter $\beta = 8\pi p/B^2 \approx 3{,}5 \times 10^4 >> 1$ for $B = 100$ G

Solar plasma beta

$$\beta = \frac{8\pi n_e k_B T}{B^2} = \frac{p_{gas}}{p_{mag}}$$

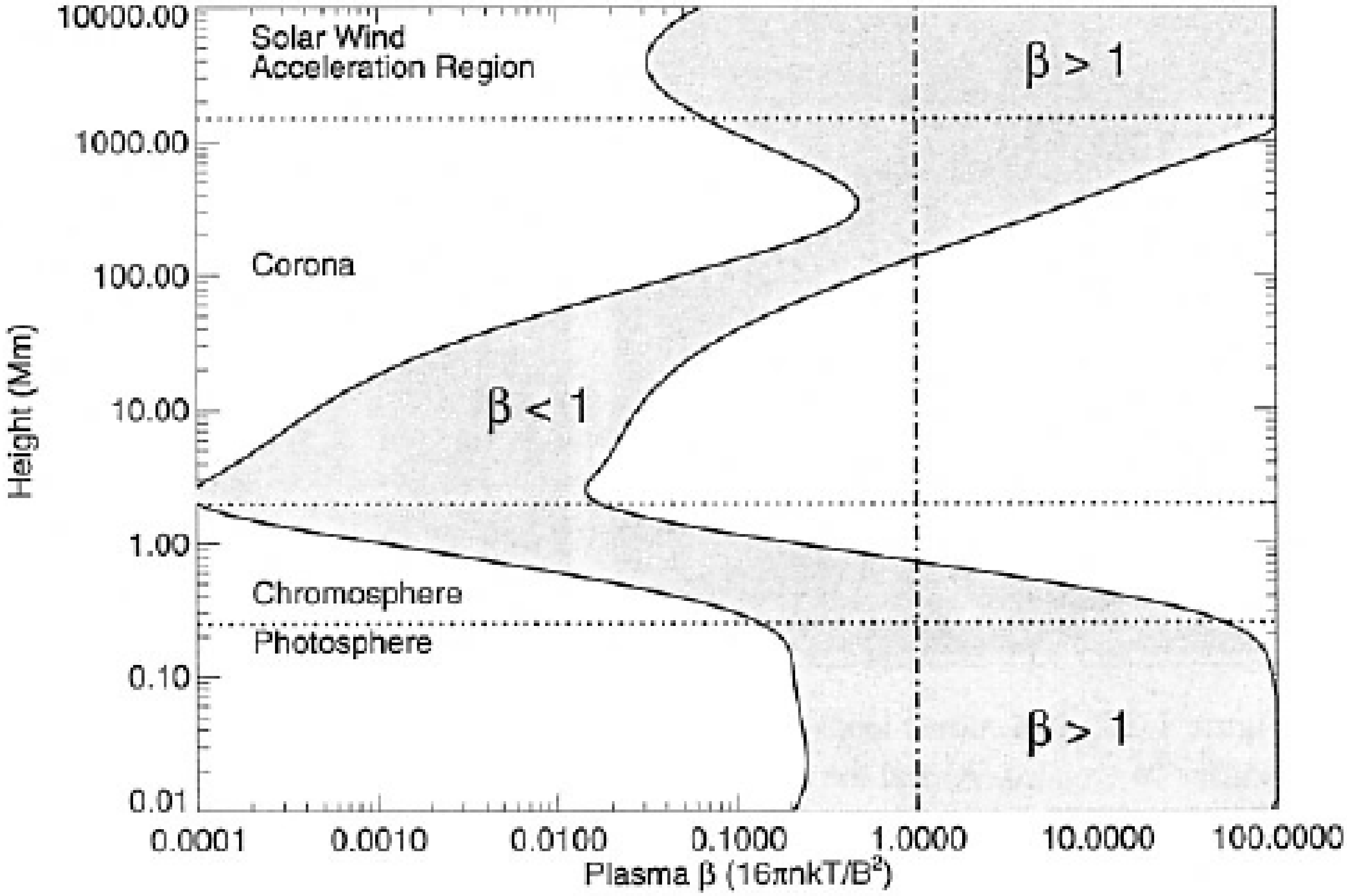

Figure 1.22: Plasma β in the solar atmosphere for two assumed field strengths, 100 G and 2500 G. In the inner corona ($R \lesssim 0.2 R_\odot$), magnetic pressure generally dominates static gas pressure. As with all plots of physical quantities against height, a broad spatial and temporal average is implied (Gary, 2001).

Anisotropy measurements in the solar wind

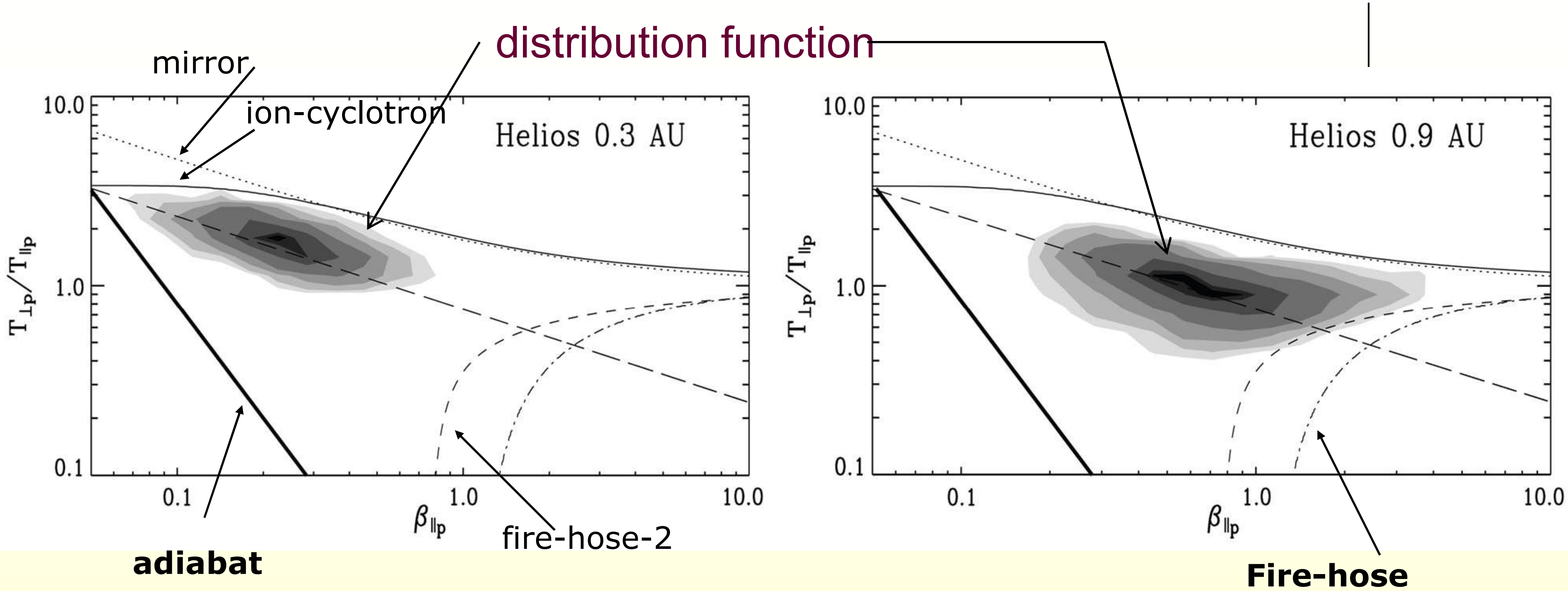

At those distances from the Sun, where there are local measurements, they show a marked anisotropy of the proton temperature plasma of the solar wind.

Background of the temperature anisotropy

Temperature anisotropy of the magnetized plasma of the solar corona and the solar wind is the result of different processes, which include, for example, the well-studied in the physics of laboratory and space plasma processes as:

❖Adiabatic compression of the plasma with a magnetic field (transverse magnetic compression tubes and loops, magnetic clouds, etc.), which results in the strengthening of the magnetic field. Owing to the conservation of the adiabatic invariant of the motion of particles in a changing magnetic field (the angular momentum of rotation of the particle $V_{\perp}^{2} / B = const$) there is growth the transverse velocity or transverse plasma temperature.

❖Free expansion of the plasma along the magnetic field, which is observed in such formations as open magnetic tubes and coronal holes. The decrease of the plasma density is accompanied by decreasing of longitudinal plasma pressure or its longitudinal temperature ($p_{||} B^2 / \rho^3 = const$).

Background of the temperature anisotropy

❖Particle dynamics in magnetic loops, which is equivalent to plasma confinement in a magnetic mirror, and which is accompanied by the formation of the temperature anisotropy of the particles due to leaving of the particles through the formed magnetic mirrors.

❖The injection of the plasma across the magnetic field in such phenomena as mass ejections, as well as direct impulse injection of particles along and across the magnetic field in the process of magnetic reconnection in solar flares.

The described phenomena and processes occurring near the sun, can be considered as the primary sources of the temperature anisotropy of solar plasma that continually support it at some level, providing many related to its relaxation of the dynamic plasma processes in the solar atmosphere and the solar wind. These include first of all different plasma waves and instabilities, as well as related processes of the solar plasma turbulence, coronal heating and solar wind acceleration.

Grounds of formulating the problem:

-- The condition of a strong magnetic field is satisfied:

$$\lambda_{e,i} >> r_{Be,i}, \quad \tau_{e,i} >> \tau_{Be,i}$$

The strong magnetic field with a complex topology makes the hot, almost collision-free plasma anisotropic and the applicability of the usual hydrodynamical description of the plasma is broken.

Particles rotating around the magnetic field lines are localized across the magnetic field at a distance of a Larmor radius. It means that transverse movements of the plasma in scales $L >> r_B$ can be described in the fluid approach.

-- In the longitudinal direction the plasma is "cold":

$$V_T < V_{wave}$$

-- A strong anisotropy of kinetic temperatures of protons and heavy ions is observed – hence, the full pressure is anisotropic:

$$p_\perp \neq p_\parallel$$

The kinetic equations

Boltzmann-Vlasov

$$\frac{\partial f_a}{\partial t} + \mathbf{u}\cdot\nabla f_a + \frac{1}{m_a}\left\{\mathbf{F}_a + e_a\left(\mathrm{E} + \frac{1}{c}[\mathbf{u}_a\mathbf{B}]\right)\right\}\nabla_{\mathbf{v}} f_a = \cancel{Q}(f_a)$$

\+ Maxwell equations for the electromagnetic field

$f_a(\boldsymbol{u},\boldsymbol{r},t)$ – distribution function of *a*-sort particles – not Maxwellian!

l.h.s. $\propto O(1)$ r.h.s.=Q(f) $\propto O(g)$ $g = \dfrac{1}{n\, r_D^3} \approx 10^{-6}$

The number of particles in a plasma sphere with a Debye radius of $\boldsymbol{r_D}$ is small.

Therefore collisions can be neglected,

Q=0 - collisionless plasma

Search for the solution of the kinetic equation

Different expansions around the steady distribution function for microscopic velocities (weight function) are used:

$$f(\vec{u},\vec{r},t) = f_0(\vec{u},\vec{r},t)\sum_{k,\nu} a_\nu(\vec{r},t)\, P_\nu^{(k)}(\vec{u},\vec{r},t),$$

$$f_0 = n\left(\tfrac{m}{2\pi kT}\right)^{3/2} \exp\left(-\tfrac{mu^2}{2kT}\right)$$ - Maxwellian

$$f_0 = n\left(\tfrac{m}{2\pi kT_\perp}\right)\left(\tfrac{m}{2\pi kT_\parallel}\right)^{1/2} \exp\left(-\tfrac{mu_\perp^2}{2kT_\perp} - \tfrac{mu_\parallel^2}{2kT_\parallel}\right)$$ - bi-Maxwellian

The perturbative solution based on the fast gyromotion ordering that applies when the Larmor gyration period is much shorter than any other characteristic time scales is used.

The MHD equations on the base of the 16-moments transport equations

$$\frac{d\rho}{dt} + \rho \,\mathrm{div}\, \mathbf{V} = 0, \qquad \frac{d}{dt} = \frac{\partial}{\partial t} + \mathbf{V}\cdot\nabla$$

$$\rho\frac{d\mathbf{V}}{dt} + \nabla\left(p_\perp + \frac{\mathrm{B}^2}{8\pi}\right) - \frac{1}{4\pi}(\mathbf{B}\cdot\nabla)\mathbf{B} = \rho\,\mathbf{g} +$$

$$+(p_\perp - p_\parallel)[\mathbf{h}\,\mathrm{div}\,\mathbf{h} + (\mathbf{h}\cdot\nabla)\mathbf{h}] + \mathbf{h}(\mathbf{h}\cdot\nabla)(p_\perp - p_\parallel),$$

$$\frac{d}{dt}\frac{p_\parallel \mathrm{B}^2}{\rho^3} = -\frac{\mathrm{B}^2}{\rho^3}\left[\mathrm{B}(\mathbf{h}\cdot\nabla)\frac{S_\parallel}{\mathrm{B}} + \frac{2S_\perp}{\mathrm{B}}(\mathbf{h}\cdot\nabla)\mathrm{B}\right],$$

$$\frac{d}{dt}\frac{p_\perp}{\mathrm{B}\rho} = -\frac{\mathrm{B}}{\rho}(\mathbf{h}\cdot\nabla)\frac{S_\perp}{\mathrm{B}^2}$$

Two adiabatic invariants are truncated by heat transport

$$\frac{d}{dt}\frac{S_\parallel \mathrm{B}^3}{\rho^4} = -\frac{3p_\parallel \mathrm{B}^3}{\rho^4}(\mathbf{h}\cdot\nabla)\frac{p_\parallel}{\rho}$$

$$\frac{d}{dt}\frac{S_\perp}{\rho^2} = -\frac{p_\parallel}{\rho^2}\left[(\mathbf{h}\cdot\nabla)\frac{p_\perp}{\rho} + \frac{p_\perp}{\rho}\frac{p_\perp - p_\parallel}{p_\parallel \mathrm{B}}(\mathbf{h}\cdot\nabla)\mathrm{B}\right]$$

$$\frac{d\mathbf{B}}{dt} + \mathbf{B}\,\mathrm{div}\,\mathbf{V} - (\mathbf{B}\cdot\nabla)\mathbf{V} = 0, \qquad \mathrm{div}\,\mathbf{B} = 0, \qquad \mathbf{h} = \frac{\mathbf{B}}{\mathrm{B}}$$

Variables and number of equations

$$\rho,\ \mathbf{V},\ p_{\perp},\ p_{\|},\ S_{\perp},\ S_{\|},\ \mathbf{B}$$ = *11 variables*

Number of equations = 11:

- The equation of a mass continuity - 1
- The equations of motion - 3
- The equations of energy - 2
- The equations for heat fluxes - 2
- The equations for a magnetic field - 3

Initial state

$\partial/\partial t = 0, \;\; \partial/\partial r = 0 \,, \; g = 0$

$$\rho_0,\; B_0,\; p_{\|0},\; p_{\perp 0},\; S_{\|0},\; S_{\perp 0},\; \mathrm{v}_0 = const$$

$V_0 \;||\; B_0,$

$S_{||0} \approx (3/2)\, n_e k_B T_{||} V_0\, \delta \;\; = (3/4)\, p_{||} V_0\, \delta$

$S_0 \approx (3/4)\, p\, V_0\, \delta$

The parameter δ is defined by the initial distribution function. Calculations of realistic distribution functions and their comparison with the observed solar wind parameters gives:

δ = 4÷0.1 (for B = 0.1÷100 G) (Hollweg, 1974, 1976).

The linear wave equations and the parameters of the problem

$X(r, t) = X_0 + X'(\mathbf{r},t)$, $X'(\mathbf{r},t) = X' \exp(i\mathbf{kr} - i\omega t)$

Parameters of the problem:

$$\omega = \omega_R + i\omega_i \,, \quad X' \propto \exp(\omega_i\, t)$$

$\alpha = \dfrac{p_\perp}{p_\parallel} = \dfrac{T_\perp}{T_\parallel}$ - Parameter of pressure anisotropy

$\beta = \dfrac{B^2}{4\pi\, p_\parallel} = \dfrac{\mathrm{V}_\mathrm{A}^2}{c_\parallel^2}$ - Magnetic field parameter (inverse to β_{plasm})

$\gamma = \dfrac{S_\parallel}{p_\parallel c_\parallel} = \dfrac{S_\perp}{p_\perp c_\parallel} \approx \delta \dfrac{\mathrm{v}_0}{c_\parallel}$ - Heat flux parameter

$l = \cos^2\theta$ - propagation angle parameter

Usual isotropic MHD theory

$$\left(\frac{\omega}{k}\right)^2 = V_A^2 \cos^2\theta$$ ***Alfvén waves***

Slow and fast magnetosonic waves

$$2\left(\frac{\omega}{k}\right)^2 = V_A^2 + c_s^2 \pm \sqrt{\left(V_A^2 + c_s^2\right)^2 - 4V_A^2 c_s^2 \cos^2\theta}$$

$$V_{slow} \le V_A \le V_{fast}$$

This parity between the phase speeds is always satisfied

These modes in the considered model are always stable!

16-moments MHD theory

$$\left(\frac{\omega}{k}\right)^2 = V_A^2 \left(1 - \frac{p_\parallel - p_\perp}{2\, p_{mag}}\right) \cos^2\theta$$

Alfvén fire hose modes – prototype of usual Alfvén waves

Fire hose instability condition:

$$p_\parallel > p_\perp + 2 p_{mag}$$

- Two modified mirror modes + two new thermal modes are described by the dispersion equation of 8-th order:

$$c_8 V^8 + c_6 V^6 + c_4 V^4 + c_2 V^2 + c_0 + \gamma \left(c_7 V^7 + c_5 V^5 + c_3 V^3 + c_1 V_1\right) = 0$$

$$V = V_{ph} = \frac{\omega}{k\, c_\parallel} \qquad c_{1\div 8} = c_{1\div 8}(\alpha, \beta, l)$$ - real functions

parameters: $\alpha = \dfrac{p_\perp}{p_\parallel}$, $\beta = \dfrac{B^2}{4\pi\, p_\parallel} = \dfrac{2}{\beta_{plasma}}$, $\gamma = \dfrac{S_\parallel}{p_\parallel c_\parallel} = \dfrac{S_\perp}{p_\perp c_\parallel}$, $l = \cos^2\theta$

MHD-wave modes in the collisionless plasma

Approach	$\pm$	
MHD	Alfvénic $\pm$ - stable Fast magnetosonic $\pm$ - stable Slow magnetosonic $\pm$ - stable	
CGL	Alfvénic fire hose $\pm$ - instability Fast mirror $\pm$ - stable Slow mirror $\pm$ - instability	
16-moments approach	$\gamma = 0$ Alfvénic fire hose $\pm$ - instability Modified fast mirror $\pm$ - stable Modified slow mirror $\pm$ - instability Fast thermal $\pm$ - stable Slow thermal $\pm$ - stable	$\gamma \neq 0$ (with heat flux) Alfvénic fire hose $\pm$ - instability Prograde fast mirror - stable Retrograde fast mirror - instability Prograde slow mirror - instability Retrograde slow mirror - instability Prograde fast thermal - stable Retrograde fast thermal - instability Prograde slow thermal - instability Retrograde slow thermal- instability

2 GOVERNING EQUATIONS of Kelvin-Helmholtz instability

In Ismayilli et al. (2018) paper we have derived wave equation:

$$\frac{d}{dx}\left(A(x)\frac{dy(x)}{dx}\right) - k^2\beta_A(x)y(x) = 0 \qquad (2.1)$$

where wave numbers $k^2 = k_y^2 + k_z^2$, $k_y^2 = k^2(1-l)$, and $k_z^2 = k^2 l$, $l = \cos^2(\theta)$, θ - wave propagation angle relatively to magnetic field directed on the z-direction.

$$A(x) = \frac{\beta_A}{\chi^2}, \quad \chi = \left(1 - l + l\frac{\beta_A}{\beta_*}\right)^{1/2},$$

$$\beta_A = \beta + \alpha - 1 - \xi^2,$$

$$\beta_* = \beta + 2\alpha + 2\alpha^2 \frac{\left(\xi^4 + 2\gamma\xi^3 + 2\gamma^2\xi^2 - 5\xi^2 - 6\gamma\xi + 3\right)}{\left(\xi^4 - 6\xi^2 - 4\gamma\xi + 3\right)\left(\xi^2 - 1\right)}, \qquad (2.2)$$

$$\xi(x) = \frac{\omega - k_z V_0(x)}{c_\parallel k_z}$$

Let $\overline{V} = \frac{1}{2}(V_{01} + V_{02})$ mean velocity, $h = \frac{V_{01}}{V_{02}} \geq 1$ jump index in velocity, $M = \frac{\overline{V}}{c_\parallel}$ Mach number, $V(x) = \frac{V_0(x)}{\overline{V}}$ normed velocity. As we have shown in Ismayilli et al. (2018) resonant interaction of the wave with the flow occurs if $\omega \approx k_z\overline{V}$. So let $\omega = k_z\overline{V}(1+\Omega)$ and Ω is unknown complex spectral parameter. Then $\xi(x) = M(\Omega + 1 - V(x))$. Instability increment (growing rate) is defined as

!

$$\Gamma = \frac{Im(\omega)}{Re(\omega)} = \frac{Im(\Omega)}{1 + Re(\Omega)} \qquad (2.3)$$

3 TANGENTIAL DISCONTINUITY

With a very narrow layer, when $L \to 0$, a tangential discontinuity arises between the flows. In this case the velocity profile may be described by the Heaviside step function of

$$V_0(x) = \begin{cases} V_{01}, & x < 0 \\ \overline{V}, & x = 0 \\ V_{02}, & x > 0 \end{cases}$$

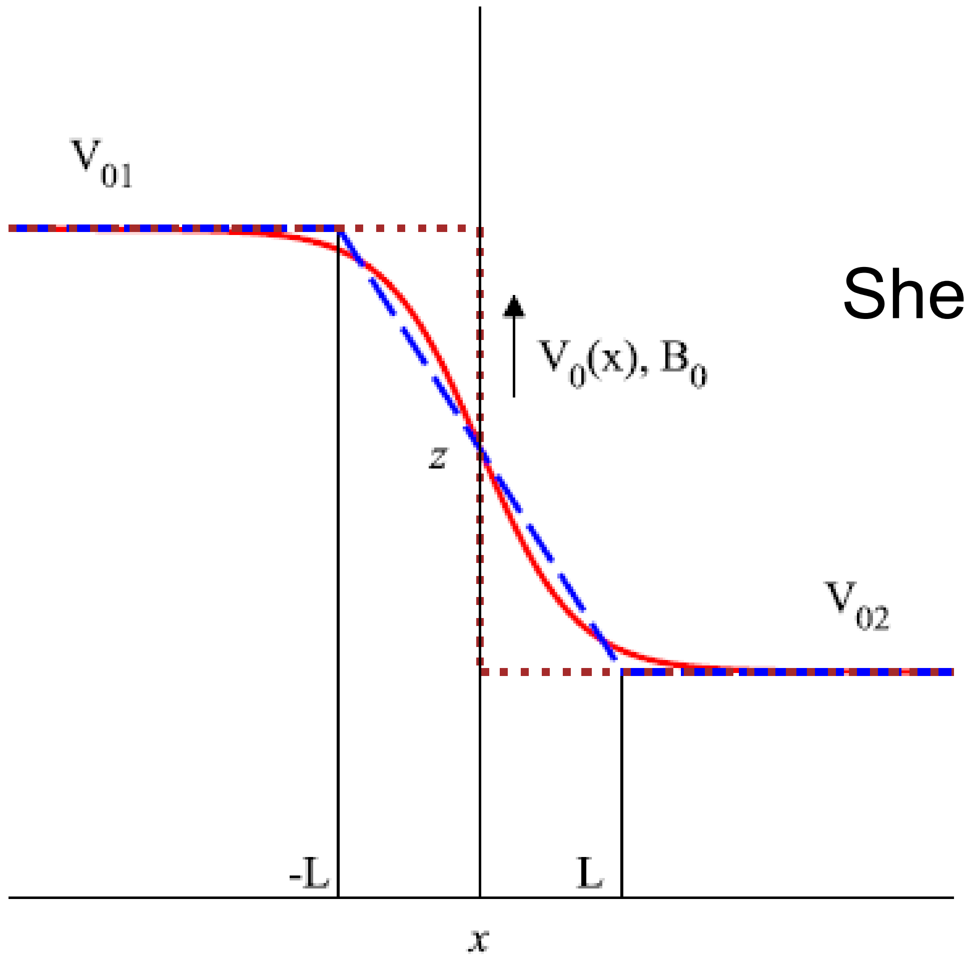

Shear layer with finite width

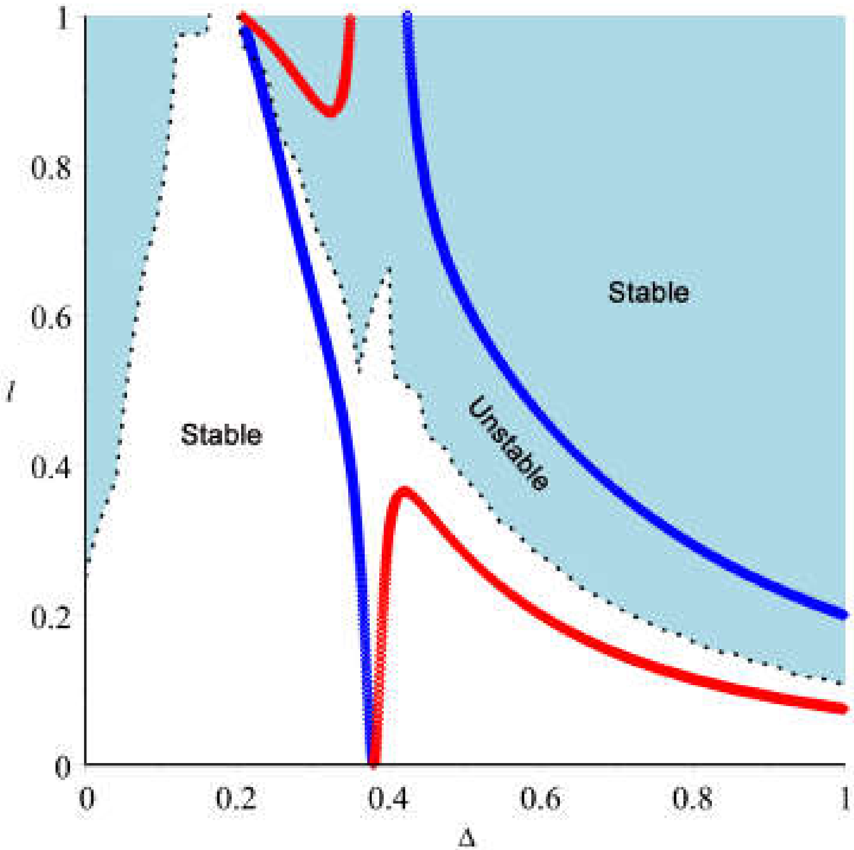

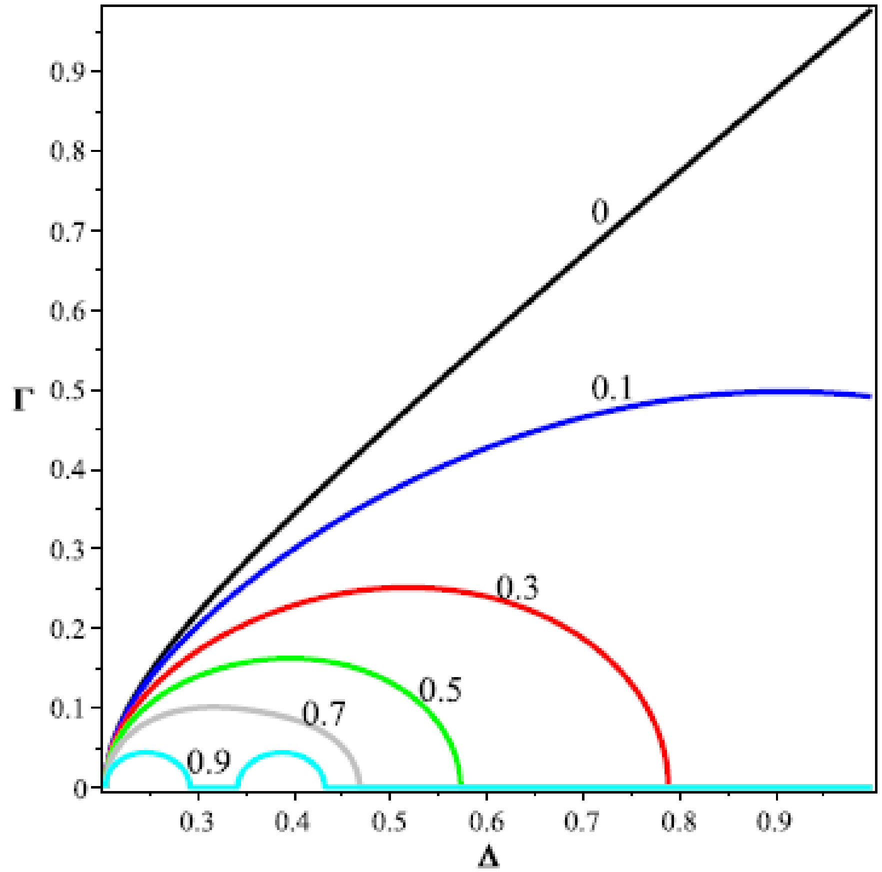

Figure 2. KHI growth rate (Γ) versus velocity shear parameter ($\Delta = (V_{01} - V_{02})/(V_{01} + V_{02})$) for a discontinuous jump in velocity. We consider different wave vector directions ($l = \cos^2\theta = 0, \ldots, 0.9$) with $l = 0$ corresponding to k parallel to the shear direction. The growth rate increases with increasing shear parameter and is maximal for $l = 0$. The calculation had Mach number $M = 6$, pressure anisotropy $\alpha = p_\perp / p_\parallel = 1.5$, inversely plasma beta ($\beta = 1$), and zero heat flux ($\gamma = 0$).

$$\Delta = \frac{V_1 - V_2}{V_1 + V_2}$$

$l \to 0$ max grows rate !

l = cos$^2\theta$
propagation angle parameter

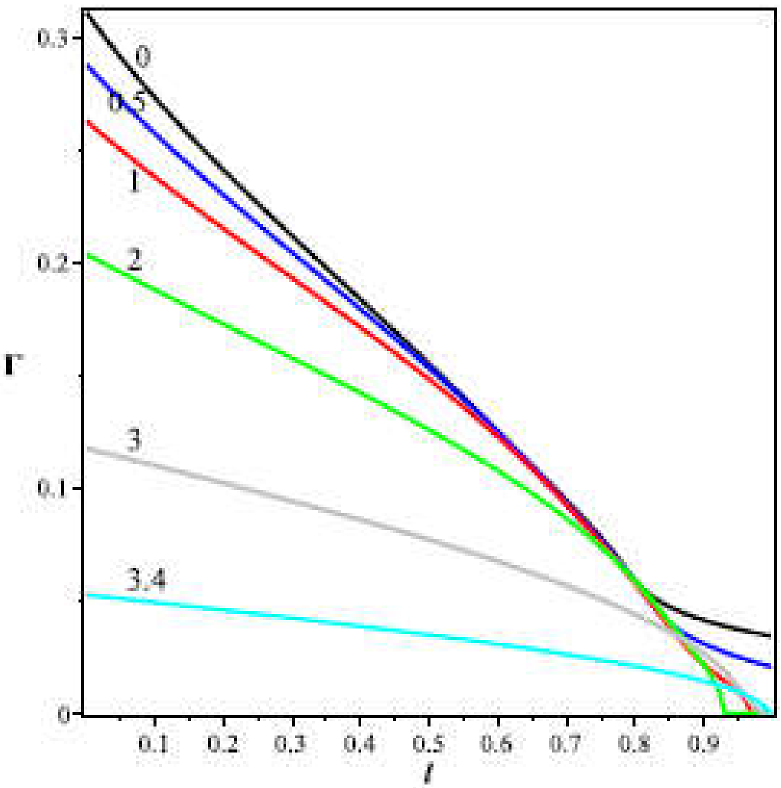

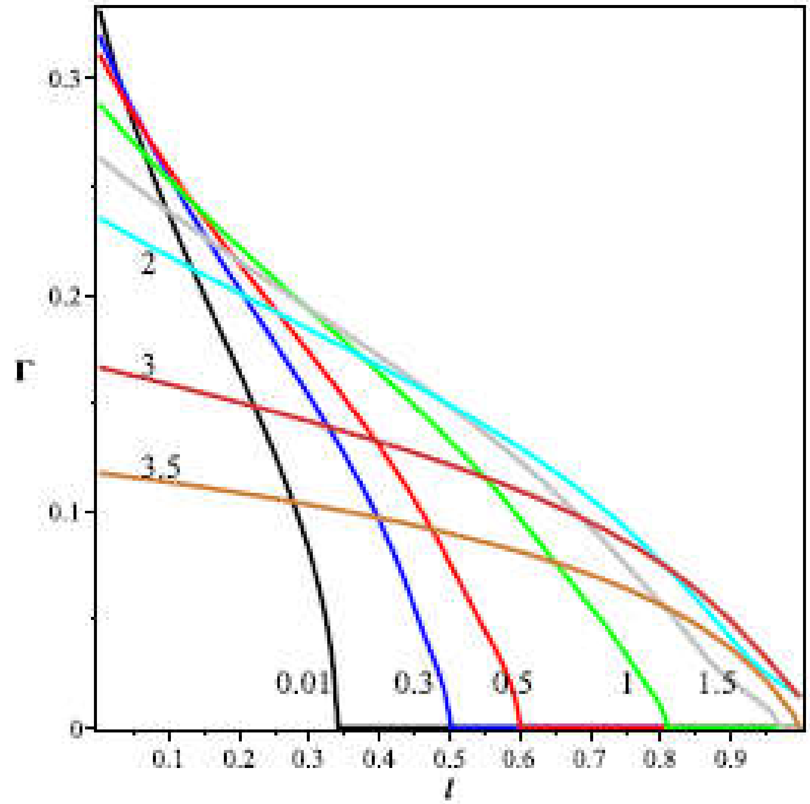

(a) Dependence of KHI Γ's growth rate on the wave propagation angle parameter relative to the magnetic field, $l = \cos^2(\theta)$. The curves indicate the values of the magnetic field parameter β for the case of Mach number $M = 6$, the strength of the shear $\Delta = 0.33$, the parameter of anisotropy $\alpha = 1.5$, and the parameter of heat flux $\gamma = 0.7$. As the magnetic field intensity increases, the KHI weakens.

4 LINEAR VELOCITY PROFILE

Let us consider the profile of the steadu flow velocity directed along the magnetic field on the z axis as

$$V_0(x) = \frac{V_{01} + V_{02}}{2} - \frac{V_{01} - V_{02}}{2} \cdot \frac{x}{L}, -L \leqslant x \leqslant L \tag{4.1}$$

Note that $V_0(-L) = V_{01}, V_0(L) = V_{02}$. For such a profile $\xi = M\left(\Omega + \Delta \frac{x}{L}\right)$. In the considered case $l = 0$, eq. (2.1) is simplified to

$$\frac{\mathrm{d}}{\mathrm{d}x}\left(\beta_A(x)\frac{\mathrm{d}y(x)}{\mathrm{d}x}\right) - k^2\beta_A(x)y(x) = 0 \tag{4.2}$$

or, we get differentiation with respect to ξ:

$$\frac{\mathrm{d}}{\mathrm{d}\xi}\left(\left(p - \xi^2\right)\frac{\mathrm{d}y(\xi)}{\mathrm{d}\xi}\right) - \varepsilon^2\left(p - \xi^2\right)y(\xi) = 0 \tag{4.3}$$

where $p = \alpha + \beta - 1, \varepsilon = \frac{kL}{M\Delta}$. Analytical solutions to this equation are expressed by the Heun Confluent Function [...]:

$$y(\xi) = D_1 H_1(\xi) + D_2 H_2(\xi) \tag{4.4}$$

$$\begin{aligned} H_1(\xi) &= HeunC\left(0, -\frac{1}{2}, 0, -\frac{p \cdot \varepsilon^2}{4}, \frac{1 + p \cdot \varepsilon^2}{4}; \frac{\xi^2}{p}\right) \\ H_2(\xi) &= \xi \cdot HeunC\left(0, \frac{1}{2}, 0, -\frac{p \cdot \varepsilon^2}{4}, \frac{1 + p \cdot \varepsilon^2}{4}; \frac{\xi^2}{p}\right) \end{aligned} \tag{4.5}$$

Substituting here the values $\xi_{1,2} = M(\Omega \mp \Delta)$ and assuming that $\eta = \dfrac{2kL}{\Delta}\Omega$, we can get the exact solution (4.10) as

$$\eta^2 = (2kL-1)^2 - \exp(-4kL). \tag{4.11}$$

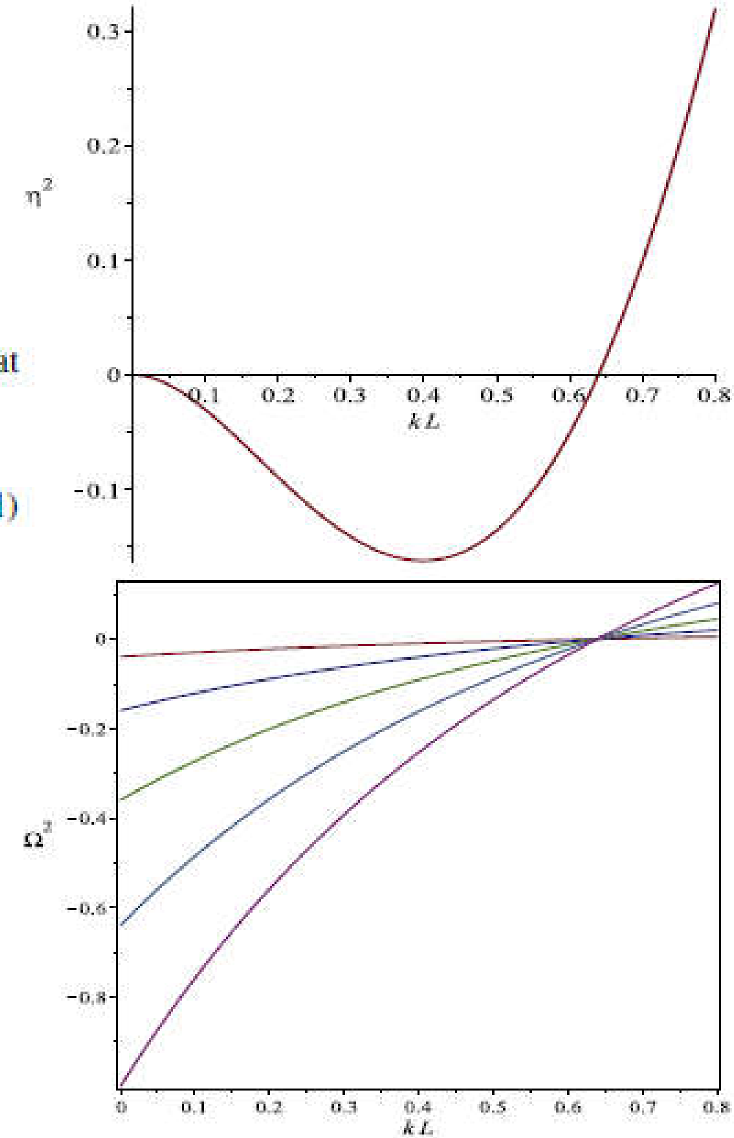

Figure 7. Dependence of the growth rate of instability on the width of the transition layer. Instability occurs when $\eta^2 < 0$. Instability condition depending on kL for different Δ. Curves from top to bottom correspond to $\Delta = [0.2, 0.4, 0.6, 0.8, 1.0]$

5 HYPERBOLIC VELOCITY PROFILE

Let us now consider a hyperbolic velocity profile that smoothly describes the transition zone between flows. Let be

$$V_0(x) = \frac{V_{02}e^{\sigma x} + V_{01}e^{-\sigma x}}{e^{\sigma x} + e^{-\sigma x}} \tag{5.1}$$

where the parameter $\sigma > 0$ describes the width of the transition zone, $L \sim 1/\sigma$. Normalized velocity $V(x) = V_0(x)/\overline{V} = 1$ at $x = 0$. For such a velocity profile, the variable $\xi(x) = M(\Omega + 1 - V(x))$ varies continuously. It is convenient to enter instead of the coordinate x

where $\varepsilon = (h-1)(k/\sigma) > 0$. This equation cannot be analytically solved in general form. In case $l \to 0$ it goes to

$$\left(t^2 - \Delta^2\right)\frac{d}{dt}\left|\left(p - (\Omega - t)^2\right)\left(t^2 - \Delta^2\right)\frac{dy(t)}{dt}\right| - \\ -\varepsilon^2\left|p - (\Omega - t)^2\right| y(t) = 0 \tag{5.3}$$

where $p = (\alpha + \beta - 1)/M$. Eq. (5.3) remains difficult for analytical study due to singularities. However, in the special but important case $p = 0$ this equation can be reduced to the Heun equation [...], the solutions of which are

$$y(t) = \frac{1}{\Omega - t}\left[C_1 H_1(t)\left(\frac{\Delta + t}{\Delta - t}\right)^{\frac{\varepsilon}{2\Delta}} + C_2 H_2(t)\left(\Delta^2 - t^2\right)^{-\frac{\varepsilon}{2\Delta}}\right] \tag{5.4}$$

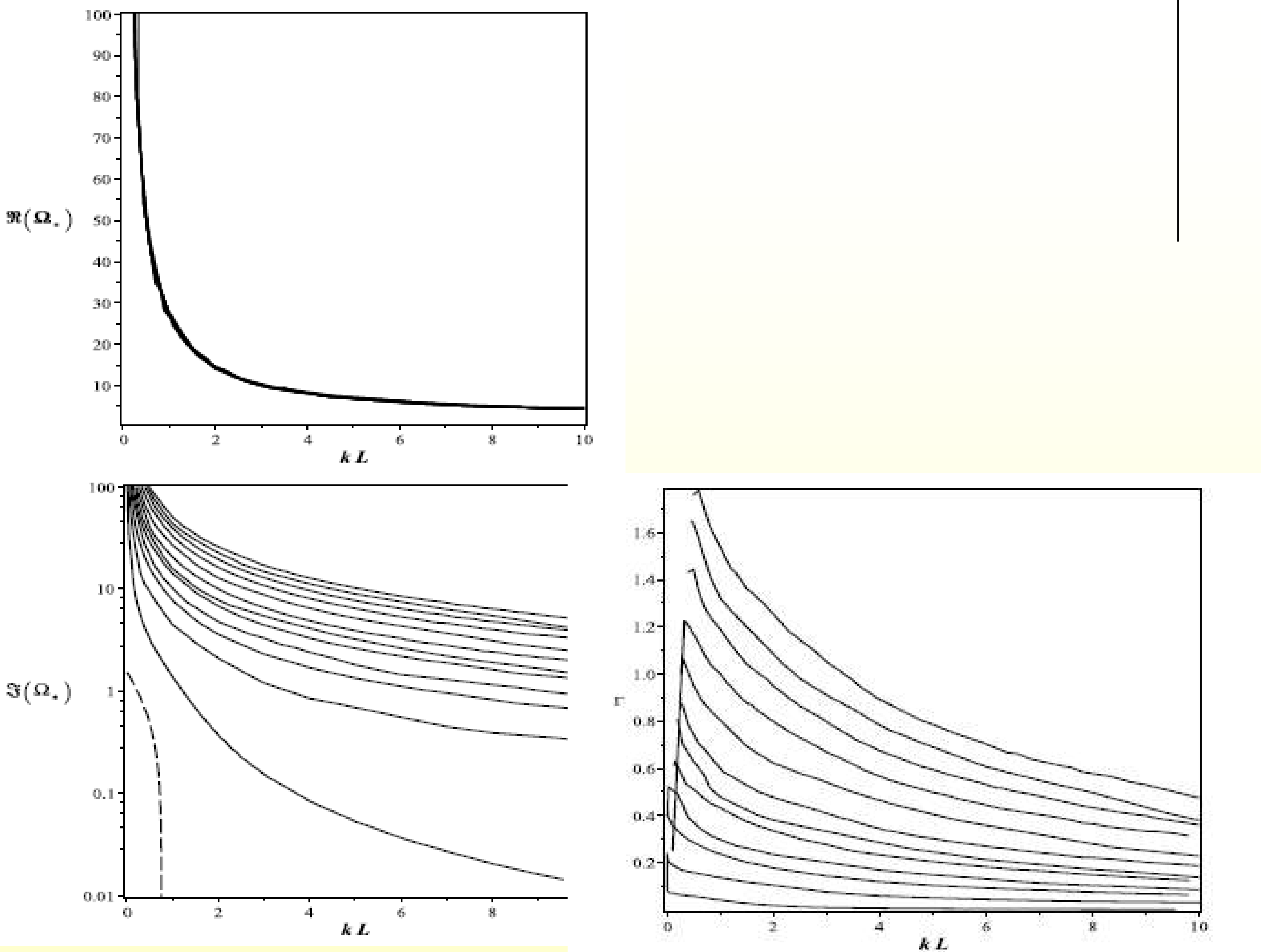

Figure 8. from top to down 1. Real parts of solutions 2. Imaginary parts of solutions 3. Growth rates of wave modes

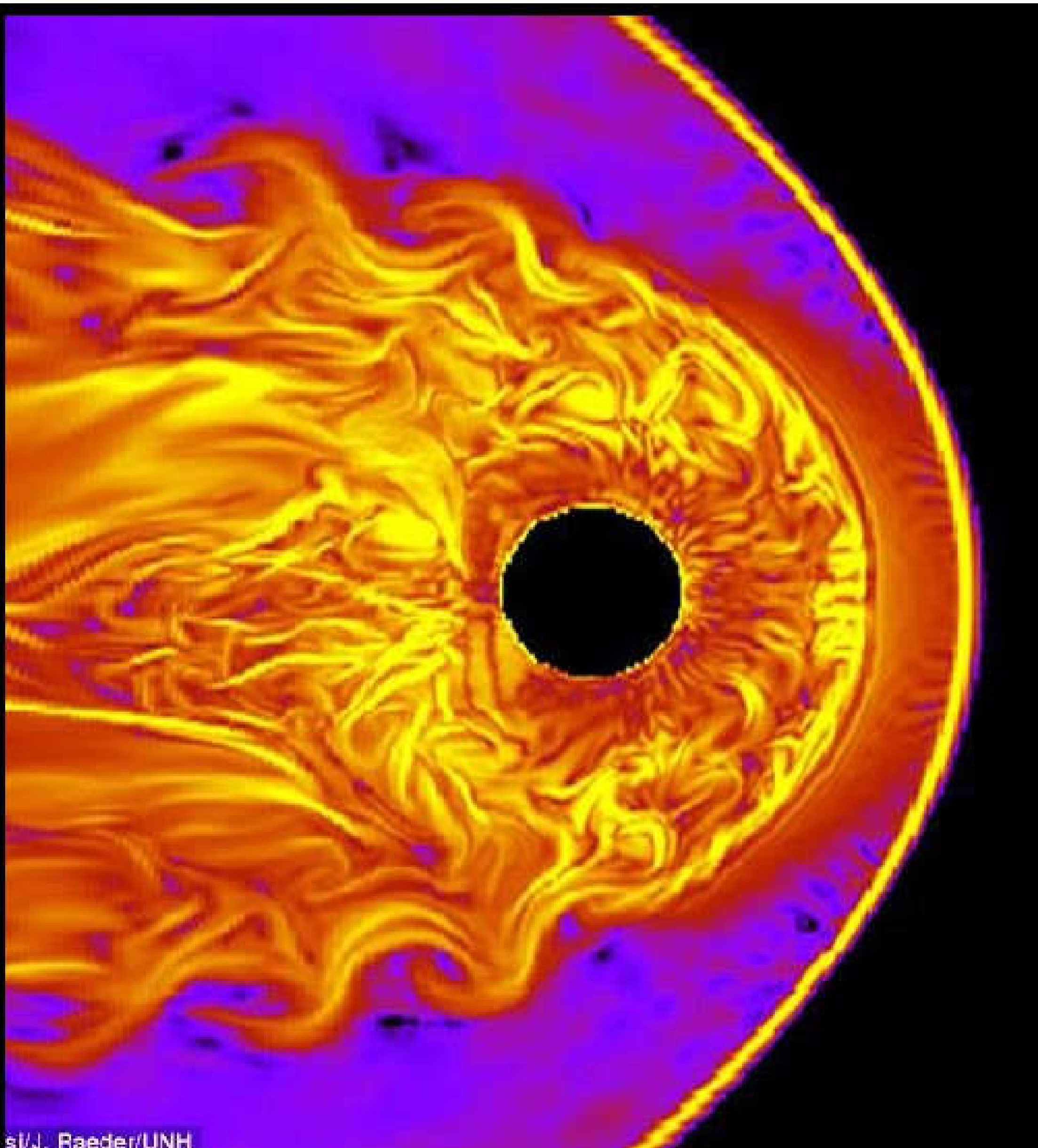

WHY IS IT IMPORTANT?

- The KHI provides a mechanism to allow plasma to cross magnetospheric boundaries.
  - MASS:
    - It enables highly efficient ion mixing across a boundary (Fujimoto & Terasawa 1994)
  - ENERGY:
    - It can generate ULF waves that can accelerate electrons in the radiation belts (Atkinson & Watanabe 1966)
    - It drives turbulent boundary layers, causing turbulent dissipation of energy. (Johnson et. al. 2014)
  - MOMENTUM:
    - It might drive large scale convection at the magnetopause, explaining the "anomalous diffusion" of momentum from the solar wind into the magnetosphere (Miura 1984)

Thanks for attention !